Science of the Total Environment 908 (2024) 168236

Contents lists available at ScienceDirect

Science of the Total Environment

journal homepage: www.elsevier.com/locate/scitotenv

Mitigating tire wear particles and tire additive chemicals in stormwater with permeable pavements

Chelsea J. Mitchell [a,1], Anand D. Jayakaran [b,*,1]

[a] School of the Environment, Puyallup Research and Extension Center, Washington State University, 2606 W Pioneer Ave, Puyallup, WA 98371, USA
[b] Extension and Washington Stormwater Center, Puyallup Research and Extension Center, Washington State University, 2606 W Pioneer Ave, Puyallup, WA 98371, USA

HIGHLIGHTS

- Permeable pavements were studied for their ability to treat tire particles and leachable tire chemicals.
- Permeable pavements retained >96 % of deposited cryomilled tire particle mass.
- Permeable pavements reduced leachable tire chemical mass by 14–100 % but exported NCBA and BTR.
- Mean mass reduction of 6PPDQ by permeable pavements was 68 %.
- Permeable pavements may be a viable strategy for intercepting tire-associated pollution generated on roadways.

GRAPHICAL ABSTRACT

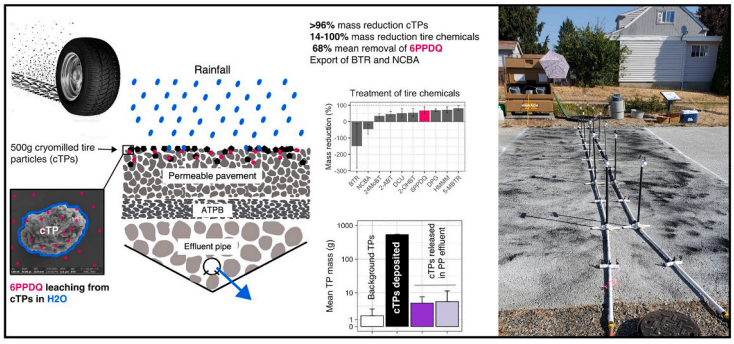

ARTICLE INFO

Editor: Jianmin Chen

Keywords:
Stormwater
Permeable pavements
Tire wear particles
Green stormwater infrastructure
6PPD-quinone
Microplastics

ABSTRACT

6PPD-quinone (6PPDQ) is a recently discovered chemical that is acutely toxic to coho salmon (*Oncorhynchus kisutch*) and can form via environmental exposure of 6PPD, a compound found extensively in tire wear particles (TWPs). TWPs deposited on roads are transported to aquatic ecosystems via stormwater, contributing to microplastic pollution and organic contaminant loads. However, little is known about the fate of TWPs and their leachable contaminants in these systems. We conducted three experiments at a high school in Tacoma, Washington, to quantify the treatment performance of permeable pavement (PP) formulations, a type of green stormwater infrastructure (GSI), for TWPs and ten tire-associated contaminants, including 6PPDQ. The PPs comprised concrete and asphalt, with and without cured carbon fibers, to improve the mechanical properties of PPs. Pavements were artificially dosed and had underdrains to capture effluent. Three experiments were conducted to evaluate PP mitigation of tire-associated pollution using cryomilled tire particles (cTPs). The 1st and 3rd experiments established a baseline for TWPs and contaminants and assessed the potential for continued pollutant release. During experiment 2, cTPs were applied to each pavement. Our results showed that the PPs attenuated >96 % of the deposited cTPs mass. An estimated 52–100 % of potentially leachable 6PPDQ was removed by the PP systems between the influent and effluent sampling stations. Background 6PPDQ concentrations in effluents ranged from 0 to 0.0029 μg/L. Effluent 6PPDQ concentrations were not explained by effluent TWP concentrations in experiments 1 or 2 but were significantly correlated in experiment 3, suggesting that

* Corresponding author at: Puyallup Research and Extension Center, 2606 W Pioneer Ave, Puyallup, WA 98371, USA.
E-mail address: anand.jayakaran@wsu.edu (A.D. Jayakaran).
[1] Puyallup Research and Extension Center, 2606 W Pioneer Ave, Puyallup, WA 98371, USA.

https://doi.org/10.1016/j.scitotenv.2023.168236
Received 21 July 2023; Received in revised form 10 October 2023; Accepted 29 October 2023
Available online 7 November 2023

leaching of 6PPDQ from TWPs retained in the pavement was minimal during a subsequent storm. Our results suggest that PPs may be an effective form of GSI for mitigating tire-associated stormwater pollution. The improved strength offered by cured carbon fiber-amended pavements extends PP deployment on high-traffic roadways where tire-associated pollution poses the greatest environmental risk.

1. Introduction

Worldwide, surface waters draining from urban landscapes show consistent symptoms of ecological degradation, known collectively as the Urban Stream Syndrome (Meyer et al., 2005; Walsh et al., 2005). These symptoms include larger runoff volumes, flashier stream hydrographs, altered channel morphology, reduced biotic richness, and increased levels of nutrients and contaminants (Walsh et al., 2005). Stormwater runoff is the primary driver of the Urban Stream Syndrome and the consequence of large runoff volumes and associated pollutants being transported rapidly from impervious surfaces to the nearest receiving water body (Vietz et al., 2016). This transport occurs via traditional but efficient drainage networks designed to quickly move water off the landscape (Walsh et al., 2005).

An acute symptom of Urban Stream Syndrome plaguing riverine ecosystems in the Pacific Northwest is the recurrent die-offs of coho salmon (*Oncorhynchus kisutch*) spawners in urban streams before they can spawn. Known as Urban Stream Mortality Syndrome (URMS), this phenomenon has been linked to a newly discovered chemical, 6PPDQ-quinone {6PPDQ; 2-anilino-5-[(4-methylpentan-2-yl)amino]cyclohexa-2,5-diene-1,4-dione}, found to be a transformation product of the anti-ozonant, 6PPD, which is widely used in tires and other rubber products (Tian et al., 2021). With an LC_{50} of 95 ng/L for coho salmon, 6PPDQ is now considered among the most toxic contaminants with EPA Aquatic Life Criteria (Tian et al., 2022). Most other contaminants with similar toxicity to aquatic species are organophosphates and organochlorines, which are pesticides specifically designed to be toxic (Tian et al., 2022). In addition, recent improvements in non-target analyses have identified other tire-associated chemicals (Peter et al., 2018; Du et al., 2020), which have since been detected in stormwater (Challis et al., 2021; Rauert et al., 2022), receiving waters (Johannessen et al., 2021), and fish tissues (Du et al., 2020).

Tire wear particles (TWPs) have emerged as a significant environmental concern as scientists increasingly become aware of their contributions to microplastic emissions (Kole et al., 2017) and their release of toxic chemicals (Challis et al., 2021; Tian et al., 2021). TWPs are generated by the abrasion of tread on road surfaces, making them a byproduct of regular tire use. In the US, an estimated 1.52 million tons of TWPs are generated annually (Kole et al., 2017). It is estimated that TWPs contribute approximately 30 % of the primary microplastics, plastics released into the environment as small particles, in the ocean globally (Boucher and Friot, 2017) and make 5–10 % of all microplastics in the ocean globally (Kole et al., 2017). Due in part to their broad range of particle sizes, the fate and transport of TWPs can vary, resulting in contamination of soils, surface water, and air (Baensch-Baltruschat et al., 2020). TWPs often melt during abrasion on the road surface, combining with road dust and other materials to create agglomerates known as tire and road wear particles (TRWP) (Baensch-Baltruschat et al., 2020). Because TWRP contain minerals from pavement aggregates, they typically are denser than simple tire rubber (Baensch-Baltruschat et al., 2020).

TWPs accumulate on roadways and parking lots and are readily transported by runoff from these impervious surfaces during rain events (Baensch-Baltruschat et al., 2020). Stormwater runoff is the main pathway for releasing TWPs into surface waters (Werbowski et al., 2021). Microplastic studies have repeatedly found that “black rubbery fragments” dominate stormwater samples (Ziajahromi et al., 2020; Werbowski et al., 2021; Zhu et al., 2021). These fragments were either presumed to be TWPs (Werbowski et al., 2021) or were determined to be TWPs via Fourier-transformed infrared spectroscopy (Ziajahromi et al., 2020) or by Pyrolysis Gas Chromatography-Mass Spectrometry (Parker-Jurd et al., 2021). Other methods to identify microplastics in water include visual identification and microscopy (Hidalgo-Ruz et al., 2012), Raman spectroscopy (Tagg et al., 2015), fluorescent staining with Nile Red (Maes et al., 2017), and thermal analysis (Renner et al., 2019).

The release of TWPs via stormwater presents a significant concern for environmental managers because TWPs are ubiquitous and a source of several chemicals to aquatic organisms (Wik, 2007; Capolupo et al., 2020; Brinkmann et al., 2022).

Green Stormwater Infrastructure (GSI) decentralizes stormwater treatment to restore pre-development hydrological processes through infiltration and evapotranspiration (Ebrahimian et al., 2019; Ebrahimian et al., 2020) and promotes pollutant mitigation through physico-chemical (Li and Davis, 2008; Jayakaran et al., 2019; Sharma and Malaviya, 2021) and biological processes (Pratt et al., 1999; Newman et al., 2006; LeFevre et al., 2012). Certain types of GSI, such as bio-retention systems, have demonstrated the ability to limit the toxicity of stormwater to coho salmon (*Onchorhyncus kisutch*) and zebrafish (*Danio rerio*) (McIntyre et al., 2014; McIntyre et al., 2015; McIntyre et al., 2016). Other studies have shown that certain GSIs can remove TWPs and microplastics from stormwater. For example, Smyth et al. (2021) found that black rubbery fragments, presumed to be TWPs, were retained in a stormwater bioretention cell. Ziajahromi et al. (2020) showed that synthetic rubber microplastics settle in the sediments of a stormwater floating treatment wetland. More recently, Rodgers et al. (2023) found that bioretention cells could decrease mass loadings of 6PPDQ by 10-fold, suggesting that this GSI technology can also mitigate leachable toxic chemicals associated with TWPs.

Permeable pavements (PPs) are a form of GSI that may effectively manage TWPs in stormwater. PPs are pavements that contain interconnected void spaces that let water infiltrate. They typically comprise a porous wearing layer over a gravel storage layer, allowing stormwater to drain through the pavement profile and infiltrate into underlying soils (Drake et al., 2013). Though initially implemented as a hydrological control for stormwater, recent research suggests that PPs can also remove pollutants from stormwater (Roseen et al., 2012; Jayakaran et al., 2019; Selbig et al., 2019). PPs are especially good at removing particulate pollutants, such as suspended solids, from stormwater (Jayakaran et al., 2019). This ability to retain particulate pollutants may translate to effective treatment of microplastics, such as TWPs, by similar processes. Rasmussen et al. (2023) quantified TWPs in road dust collected from permeable pavements in Denmark by a street sweeper. Based on the mass of TWPs detected via pyrolysis GC/MS, they estimated that PPs might act as a sink for TWPs in the environment.

Despite their potential to prevent road runoff and provide in situ water quality treatment, widespread deployment of PPs has been limited by their structural integrity compared to traditional pavements (Scholz and Grabowiecki, 2007). The fine particles used to create a pavement's wearing layer are screened out to build PPs, allowing interconnected void spaces to form within the pavement structure. The omission of these fine particles reduces the mechanical strength of PPs, relegating them to being used primarily in parking lots, sidewalks, and driveways (Scholz and Grabowiecki, 2007; Roseen et al., 2012). One approach to strengthening PPs is amending them with additives, like certain fibers, that improve mechanical properties while maintaining porosity (Gupta et al., 2019; Bright Singh and Madasamy, 2022). Recently, researchers and engineers have taken advantage of cured carbon fiber composite materials (CCFCMs), a byproduct of the airplane manufacturing process,

as strengthening amendments for PPs (Rangelov et al., 2016; Rodin et al., 2018; Zhang et al., 2019; Nassiri et al., 2021). CCFCMs have been shown to increase tensile, compressive, and flexural strength (Rangelov et al., 2016; Rodin et al., 2018) and improve pervious concrete's freeze-thaw durability (Nassiri et al., 2021). CCFCMs also increased indirect tensile strength and cracking resistance in porous hot mix asphalt (Zhang et al., 2019). With increasing development pressure and limited spaces for GSI in densely populated urban areas, the wider-spread application of PPs for high-traffic roads could address a latent demand for GSI.

1.1. Study design and objectives

Given that PPs have a proven track record of suspended sediment and other particulates removal (Jayakaran et al., 2019), we hypothesized that PPs would retain the majority of deposited TWPs. We also expect that PPs mitigate some contaminant release through adsorption to internal surfaces within the pavement. However, because retained TWPs are in contact with water in the pavement's pore spaces during subsequent storms, we hypothesized that TWPs retained within the pavements would continue to leach contaminants after being rewetted in subsequent storms. Therefore, this study's overarching goal was to evaluate the potential for permeable pavements to mitigate tire-associated pollution, including TWP microplastic pollution and harmful leachable contaminants such as 6PPDQ.

To determine the treatment potential of permeable pavements for tire particles and leachable tire chemicals, three experiments were carried out at four permeable pavements at a high school field site in August 2021. The tire particle and chemical mass transport rates were quantified for four different lined sections of asphalt and concrete permeable pavements with and without CCFCMs. Specific objectives for the three experiments were: A) establish particles and chemical baseline concentrations attributable to parking lot traffic, B) quantify the movement of deposited particles and associated chemicals through permeable pavements, and C) quantify post-deposition movement of particles and chemical through pavements.

1.2. Study limitations and novelty

- We used cryomilled tire particles (cTP) as an idealized form of TRWPs for their consistent size and ease of identification. Still, it is essential to note that there are density and morphological differences between the two and possibly subtle differences in fate and transport. When tire particles are generated in the environment, they often become agglomerated with bits of road wear comprising tire rubber (50–80 %) and mineral dust from road surfaces (20–50 %), yielding a higher density (1.3–1.9 g/cm^3) than tire tread rubber (1.2 g/cm^3) (Wagner et al., 2022). This density difference between cTPs and TRWPs is that heavier TRWPs would be more likely to settle out of water moving through the pavements.
- Each study pavement was dissimilar from the others both in structure and hydrologic properties. However, these were field-scale systems representing a range of likely outcomes regarding the fate and transport of cTPs and TACs.
- Only three experiments were conducted due to the constraints imposed by expensive analytical costs. We are confident that our work is representative of the physicochemical dynamics associated with an impulse of cTPs on a permeable pavement surface preceding a rainfall event. However, we cannot account for the in situ formation of 6PPDQ during the experiment.

Regarding novel outcomes, this is the first study to evaluate the removal of tire particles or tire-associated chemicals by permeable pavements. This study adds to the very limited data on tire particles and tire-associated chemical treatment by water treatment technologies. The background pollutant data in this study addresses the data gap of the tire particles and associated organic pollutants released by permeable pavements in parking lot settings. These data may be useful for the development of watershed-scale models aimed at predicting 6PPD-Q loading.

2. Methods

2.1. Pavement construction and sampling infrastructure

The permeable pavements used in this study were located at the Industrial Design Engineering and Art (IDEA) High School in Tacoma, WA, USA (N47.19606°, W122.44157°). The four pavement cells evaluated in the study were not replicates. Each pavement was uniquely constructed with different pavement materials, surface areas, and contributing areas. The pavements included porous concrete overlaying porous asphalt (hereafter, CN), porous concrete overlaying porous asphalt with CCFCMs (hereafter, CC), porous asphalt (hereafter, AN), and porous asphalt with CCFCMs (hereafter, AC) (Fig. S1). The pervious concrete cells (CN and CC) had a surface layer of pervious concrete with a short polypropylene fibers (M70) amendment. The CN pavement's base layer was asphalt-treated permeable base (ATPB), and the CC pavement's base layer was ATPB with a 0.05 % (by weight) CCFCM amendment. Porous asphalt pavements (AN and AC) both contained a surface layer of ½" porous hot mix asphalt (PHMA), and the AC pavement's PHMA was amended with 0.05 % (by weight) CCFCM amendment. The porous asphalt pavements both had an ATPB base layer.

Each pavement was outfitted with a subsurface perforated pipe or underdrain that ran the length of the pavement, collecting drainage from an 8-foot-wide section of pavement lined with an impermeable geomembrane that was situated just below the permeable ballast and above the underlying native soils (Fig. S2). This perforated pipe transported water to an outlet housed in a subsurface catch basin.

2.2. Synthetic storms and effluent sampling

Flow was estimated at the underdrain pipe's outlet using a Thel-mar weir with a pressure transducer recording stage every 5 min. Pavement effluent was sampled with automated refrigerated water samplers (Teledyne ISCO, Lincoln, NE) that collected flow-weighted samples. Every autosampler was calibrated in the field to ensure that aliquot volumes matched programmed values. Simulated storms were conducted during dry weather when the school was closed for the summer break. Typical of the warm, dry summers of the region, there was little precipitation (<2.5 mm) in the 2-month window before the simulated storms.

A series of 3 field experiments were carried out on consecutive days from August 23–25, 2021. The aim of Experiment 1 was to flush existing TWPs and associated chemicals from the pavements to establish baseline concentrations attributable to parking lot traffic. The objective of Experiment 2 was to simulate the deposition of tire particles over a 2-week dry period, followed by a first flush storm event to assess treatment by the pavements. We chose to use uniformly sized (50 μm) cryomilled tire particles (hereafter cTPs) obtained from an online retailer (Northern West Stuff) who generated these particles by cryomilling used tire treads (described by supplier as crumb rubber but confirmed by personal communication to be used tire tread) and sieving to the specified size class. cTPs were used as a surrogate for TWPs to ensure we could obtain sufficient material for dosing and to maintain a consistent particle morphology and composition. Finally, the aim of Experiment 3 was to simulate a storm occurring after a first flush storm to see if TWPs continued to mobilize through pavements and if chemicals continued to leach from TWPs trapped within pavements. A schematic of the three experiments is presented in Fig. 2.

Each experiment utilized the same pavement water dosing procedure. Municipal water from a City of Tacoma fire hydrant was used to dose the pavements via a sprinkler manifold (Fig. 1). Pavement surfaces

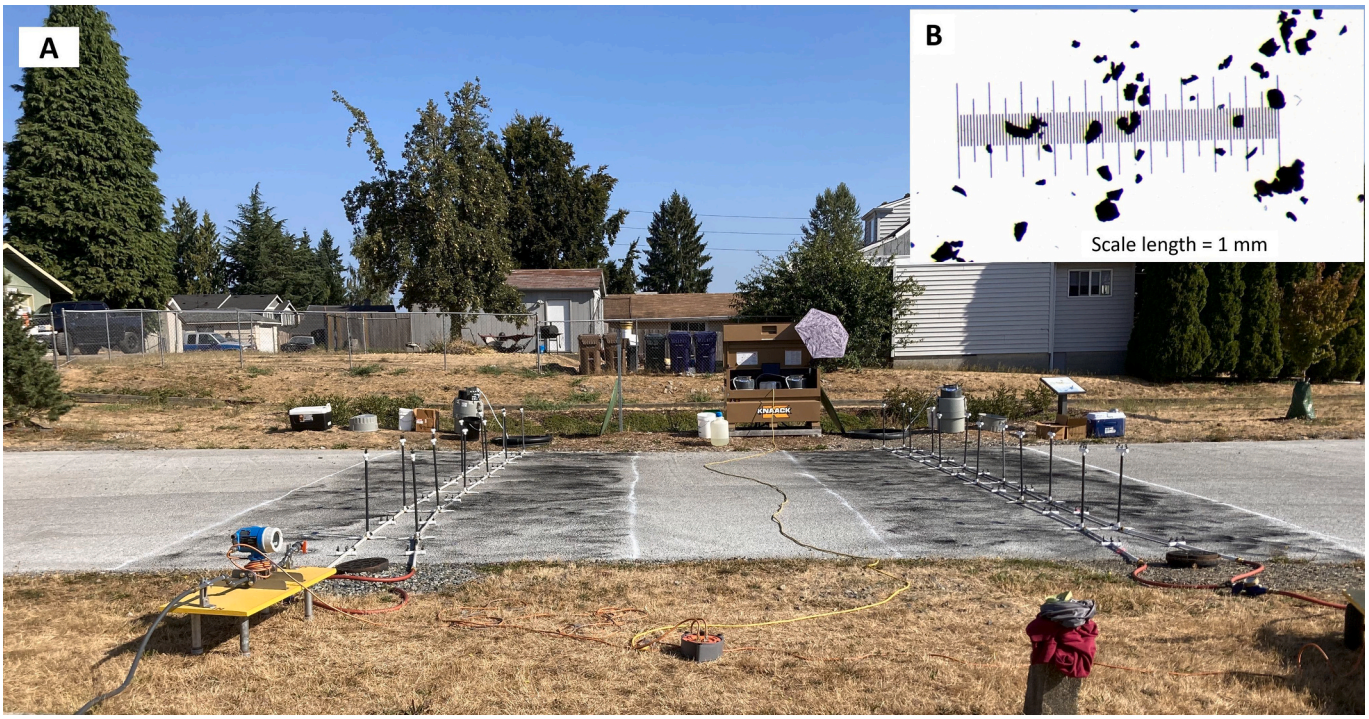

Fig. 1. Pervious concrete pavement cells (CC on the left, CN on the right) were covered in cTPs during experiment 2.

were dosed with water at a rate of 32 L/min until flow was observed from the underdrain effluent pipe (Fig. S2). Once effluent flow began, dosing continued for another 60 min, during which 13 individual flow-weighted 900 mL aliquots and one field blank were collected in separate 1 L HDPE containers using a calibrated autosampler. Flow pacing was predetermined from previous sampling efforts and estimating likely effluent volume from the effluent sample pipe over 60 min. After the autosampler collected all samples, the 13 samples were transferred to 946 mL amber glass bottles. These samples were designated for cTP analysis and henceforth called cTP-samples.

Concurrent with every cTP sample collection, another second sample was collected directly from the effluent source using a second calibrated autosampler manually triggered to collect 900 mL aliquots pumped into thirteen 946 mL amber glass bottles. This second set of samples was designated to be analyzed for tire wear chemicals, henceforth called chemistry-samples. All samples were stored on ice until transported for long-term storage at WSU Puyallup. cTP and chemical samples were stored at 4 °C and −20 °C, respectively, until analysis. All collection vessels were cleaned via sequential rinses with MilliQ water, methanol (Optima grade, CAS 67–56-1, Thermo Scientific), ethyl acetate, and methanol. HPDE ISCO bottles were cleaned with Liquinox (Alconox Inc., New York, USA) and Reverse Osmosis water before each use. All leachate and chemical analyses reported in this study were contracted to the Center for Urban Waters chemistry lab in Tacoma, WA.

2.3. cTP characterization

cTPs were imaged in two directions to their three-dimensional form (Fig. 3). Based on these images, we saw that cTPs were not plate-like but roughly spherical. A simplifying approach was to assume a nominal diameter (Wadell, 1932; Lane, 1947) for the cTP particles. Particle hydrophobicity was estimated using drop-shape analysis using a Krüss DSA 100 (Hamburg, Germany) to determine the air-water contact angle. The mean (SD) contact angle was 127.9 (1.9), indicating that these particles were strongly hydrophobic.

2.4. cTP deposition

Approximately 500 g of cTPs (Fig. 2) were dry deposited over a 32 m^2 section of each pavement (AC = 535 g, AN = 530 g, CC = 551 g, CN = 536 g). The 32 m^2 area represents the approximate area wetted by the sprinkler dosing system. The mass of cTPs deposited on each pavement was estimated based on the following assumptions: 1) The average TWP road wear emissions for 4-wheel cars is 0.132 g/vehicle/km (Kole et al., 2017); 2) Annual average daily traffic (AADT) is 30,000 vehicles/day (WSDOT traffic GeoPortal); 3) TWP emissions have been deposited for the previous 14 days without wash off by rainfall; 4) the size of the TWP deposition area (4 m × 8 m) was equivalent to an 8 m stretch of a standard US highway lane.

2.5. Laboratory analyses of cryomilled tire particle leachate

Two batches of cTP leachate were produced from the cTPs using 1) RO water and 2) municipal water collected from the same source used to dose the pavements. To generate the leachate mixture, 1 g of cTPs were mixed in 1 L stainless steel columns with 1100 g of 3 mm glass beads (pre-washed with methanol) to maximize the contact area between tire particle surfaces and water. Water (RO or municipal) was pumped via upward flow through the columns at a flow rate of 0.5 L/min for 24 h using a peristaltic pump (Tian et al., 2021).

Though the 24-h cTP leachate reflects a longer contact time for cTPs in water than the simulated storm experiments (duration 1.5–6.5 h), published studies suggest that chemicals at the surface of tire particles leach rapidly in water. Hiki and Yamamoto (2022) leached 6PPDQ from road dust, reporting that the time to reach half the equilibrium concentration was <30 min using a pseudo-first-order kinetic model. Monaghan et al. (2021) observed 6PPDQ reaching a stable state after 30 min of contact with an aqueous solution. This suggests that 6PPDQ leaches rapidly from particles well within the water contact time in this study. The implication for our study is that the contact time between cTPs and water yielded equilibrium concentrations similar to that from the 24-h leachate.

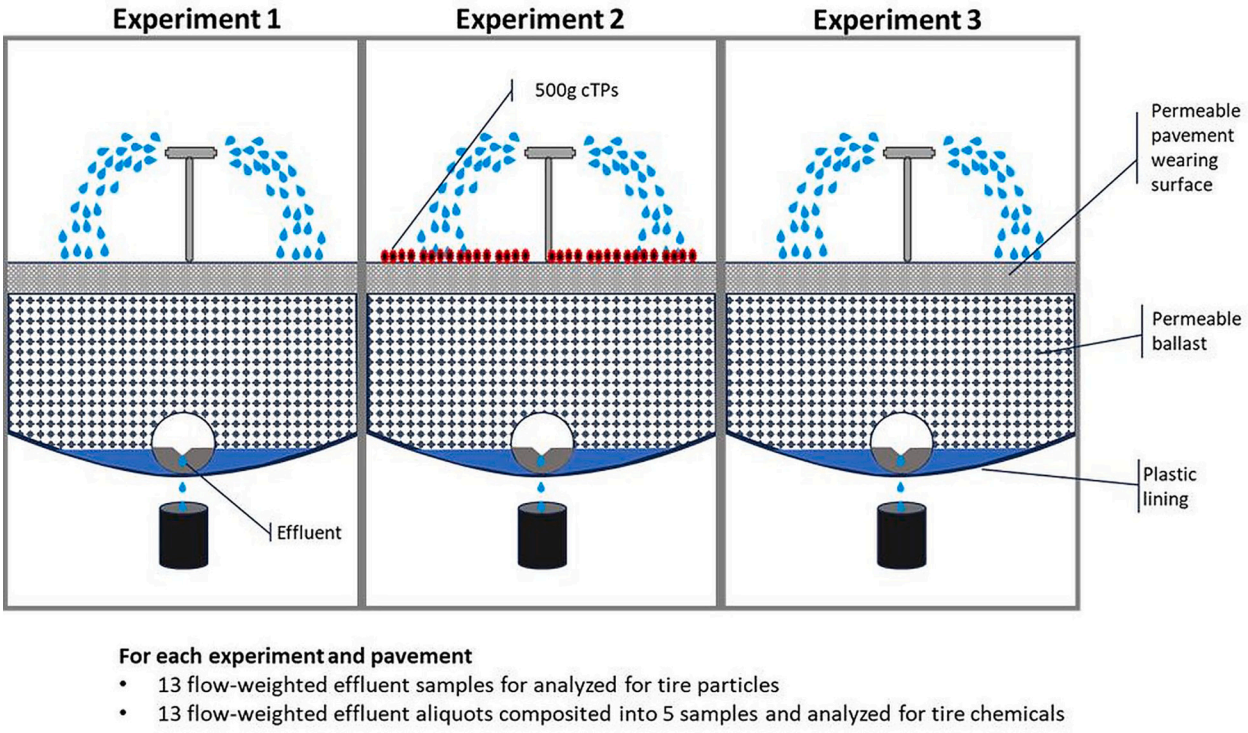

Fig. 2. Dosing of pavements over three experiments. Left - dosing with water to establish baseline. Middle - dosing with the addition of tire particles on the pavement surface. Right - dosing the pavements with just water to study post-deposition flush.

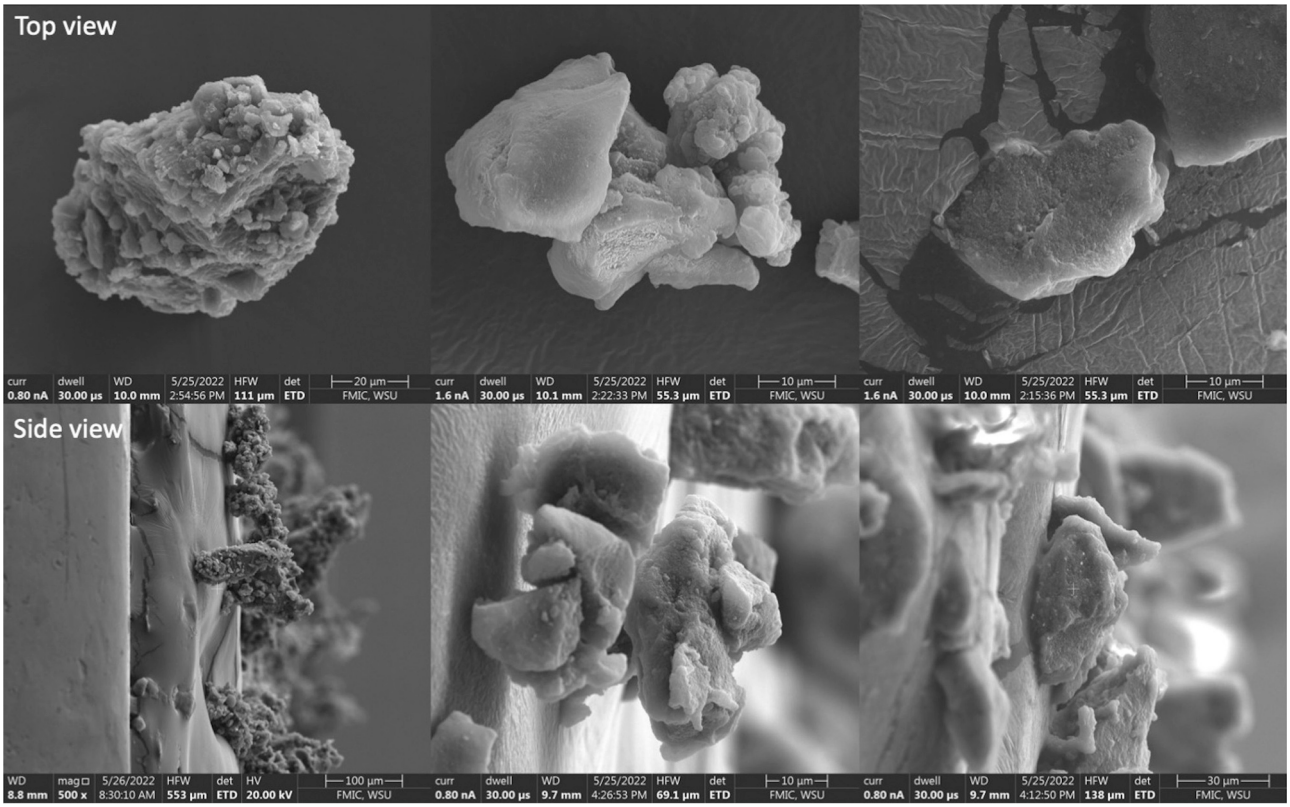

Fig. 3. Scanning electron microscopy (SEM) images of the cTPs used in this study. Top row: top view of particles. Bottom row: side view of particles.

2.6. Chemical analyses of pavement effluent

Ten tire-associated chemicals were analyzed in pavement effluent samples following methods published by Hou et al. (2019): 6PPDQ, diphenyl-guanidine (DPG), hexamethoxymethyl-melamine (HMMM), N-cyclehexyl-1,3,benzothiazole-2-amine (NCBA), benzotriazole (BTR), 5-methyl-1H-benzotriazole (5-MBTR), 2-amino-benzothiazole (2-ABT), 2-hydroxy-benzothiazole (2-OHBT), 2(4-Morpholinyl), benzothiazole (24MoBT), 1,3 dicyclohexylurea (DCU). A list of chemicals and their internal standards and detection limits can be found in the Supplemental Information Section 1 and Table S1, respectively. Effluent samples for chemical analysis were frozen at −20 °C for storage between sample collection and processing. Before sample extraction, thawed effluent samples were composited to reduce the cost of chemical analysis. The result was 5 composites spanning each pavement's effluent hydrograph during each experiment with the following compositing scheme: composite 1 = aliquot 1, composite 2 = aliquots 2–4, composite 3 = aliquots 5–8, composite 4 = aliquots 9–12, composite 5 = aliquot 13. All analytical chemistry was contracted through The Center for Urban Waters in Tacoma, WA. Composited samples were extracted via Solid Phase Extraction (SPE) using Oasis HLB cartridges (6 mL, 200 mg) and then eluted from the cartridges via 2 × 5 mL rinses with Optima LC/MS grade methanol (Fisher Scientific). Samples were concentrated to 0.9 mL via evaporation in a water bath (35 °C) under pressure from nitrogen gas (5 psi). Samples were analyzed on an Agilent 1290 chromatograph system coupled to an Agilent 6460 Triple Quadrupole (QQQ) mass spectrometry (LC-MS/MS).

2.7. cTP extraction from stormwater

A simple approach of weighing the filters before and after filtration was attempted but abandoned because our analytical equipment did not have the necessary precision to measure the low cTP masses on the filters. Instead, a density separation approach was used (adapted from Rodrigues et al., 2020). cTPs and background TWPs were extracted from effluent samples using $ZnCl_2$ solution to densify the sample (density = 1.6–1.7 g/mL, Wagner et al., 2022). Light (particles <1.6 g/cm^3) and heavy fractions (particles >1.6 g/cm^3) were filtered through glass fiber filters (47 mm) and then dried.

2.8. Quality assurance

Field blanks were analyzed for each experiment-pavement combination and cTP and TAC analyses following the same protocol as all effluent samples. Lab blanks were run using DI water for each sample batch of the cTP and TAC analyses (n = 2) following the laboratory analyses for effluent cTP and TACs. Additional lab blanks (n = 2) were run for the TACs using municipal tap water from the same source as the design water for the study. Spike and recovery samples were run for 5 samples and 6PPDQ concentrations (2, 4, 10, 40, and 50 ng/L), and results are reported in Section 1 and Table S2 of the Supplemental Information. Additional methodological details on sample QAQC is provided in Section 1 of the Supplemental Information.

2.9. Calculating mass reductions – cTPs

Dried glass fiber filters from the previous density separation step were imaged using a Nikon SMZ800 imaging microscope fitted with an Infinity 3 camera (Teledyne Lumenera, Ottowa, CA) and analyzed using ImageJ (Schneider et al., 2012). Four images were taken at random locations on each filter's surface. The tire particle count of each figure was determined in imageJ via a custom macro that converted the image to 8-bit, used a threshold determination to select only black particles, and then filtered particles by circularity (0.2–1.0) and size (20-300 μm length) to omit filaments and particles that could not be confirmed to be tire particles. This size range was determined by measurement of cTP dimensions from SEM images in ImageJ, which indicated the smallest, medium, and largest dimensions of these particles had mean lengths ranging from 42 to 84 μm. The remaining particles were then converted to outlines and counted using the ImageJ particle analysis function (Fig. 4).

The mass reduction of TWP by PP was estimated by converting TWP concentration data to a mass. First, the total number of TWPs per glass filter was calculated by extrapolating the average particle number per image area (mm^2) to the full size of the filter. We then summed the particles/filter found for each sample's light and heavy fractions to determine the number of particles in each 1 L effluent sample.

To calculate the tire particle mass in a sample, we made the following assumptions:

1. Particles were spherical with a 65 μm nominal diameter (based on mean particle diameter from SEM imaging). The manufacturer stated that the cTPs had a mean size of 50 μm. Using the formula for a sphere and assuming a diameter of 65 μm, we estimated the mean volume of each cTP to be 1.44 * 10^{-7} cm^3.
2. The density of the cTPs was 1.2 g/cm^3 (Wagner et al., 2022).
3. Therefore, the mass of each cTP particle was, on average, equivalent to 1.73 * 10^{-7} g (1.44 * 10^{-7} cm^3 * 1.2 g/cm^3).

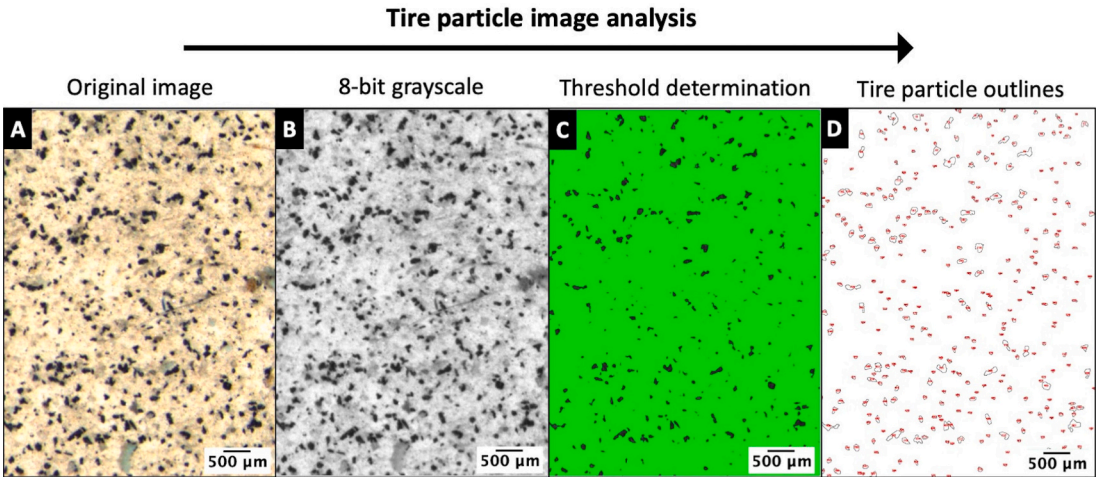

Fig. 4. Image analysis workflow for quantifying cryomilled tire particles in effluent samples. A) Image of pavement effluent sample filtered onto glass fiber filter. B) 8-bit adjustment to grayscale in ImageJ (the darkest particles are cTPs). C) Manual threshold determination in ImageJ used to select only the black particles (cTPs). D) Particle outlines, numbered (red), displaying the particles used in the particle count.

cTP concentration as a mass per unit volume of stormwater was then calculated as the product of the number of particles per unit volume of sample water and the average mass of a single cTP particle. Finally, the tire particle mass in each effluent sample was calculated as the product of cTP concentration (g/L) and the associated effluent volume (L) represented by that sample. Influent and effluent volumes were measured; however, only a fraction of the influent volume appeared in the effluent recovery underdrain (0.4–61.1) because the system was not closed. Therefore, total cTP masses for each pavement and experiment were corrected by multiplying by the ratio of influent to effluent volumes, facilitating a direct comparison of deposited and effluent masses. Mass reductions were then calculated as the difference between the mass of cTP deposited on the pavement surface and the corrected mass of cTP in the effluent. Finally, the removal efficiency was calculated by expressing the cTP mass reduction as a fraction of the mass of deposited particles.

2.10. Calculating mass reductions – tire-associated chemicals

We used data from the leachate experiment (Section 2.5) to estimate the likely concentrations of tire-associated chemicals (TAC) leached from the cTPs deposited on the pavement surface during experiment 2 (Table 1). These concentrations effectively were the influent concentration for TACs in experiment 2. A similar methodology was used by McIntyre et al. (2021) to estimate TWP mass that was likely to produce observed TAC concentrations in surface waters. Given that 1 mg of cTPs was mixed in 1 L of water to generate the tire leachate mixture in the leachate experiment, we assumed that the mass of individual TACs in 1 L of the stormwater-cTP mixture infiltrating the pavement surface could be calculated as follows:

$$TAC\ conc.in\ influent\ stormwater\ (mg/L) = a^{*}\frac{1\ mg\ cTP}{1\ L\ of\ water} \quad (2)$$

where a is a constant of proportionality equal to the ratio of the concentration of a specific TAC measured during the leachate experiment to the mass of cTPs used in the leachate experiment – which was 1 mg per liter of water (33 L total).

To calculate the mass of TAC available to be leached from the total mass of cTPs deposited on the pavements, the following equation was used:

$$Mass\ available\ to\ be\ leached\ (\mu g) = \frac{Leachate\ chemical\ mass\ (\mu g)}{1000\ \mu g\ cTPs} \times mass\ particles\ deposited\ (\mu g) \quad (3)$$

The mass of TACs in the effluent for a specific event was calculated by multiplying the concentration for each TAC in a composite sample by the volume of that composite (L) and then summing mass over all five composites for an event. Effluent TAC mass was corrected to account for lost volume, as described in Section 2.8. The mass reduction of a TAC by event was calculated by calculating the difference between influent and corrected effluent mass and expressing this difference as a fraction of the influent mass.

Table 1
Chemical concentrations measured in leachate generated from cTPs in municipal tap water at 1 μg/L. Chemical concentrations marked with a ^ were detected above the calibration curve and were deemed semi-quantified. Further dilutions of these samples did not yield quantifiable results due to the inability to detect the internal standard.

Tire-associated chemical	Leachate concentration (μg/L)	a coefficient
DCU	9^	0.009
DPG	11^	0.011
24MoBT	0.58	0.00058
2-ABT	0.38	0.00038
2-OHBT	57^	0.057
5-MBTR	0.11	0.00011
6PPDQ	0.46	0.00046
BTR	0.015	0.000015
HMMM	11^	0.011
NCBA	0.8	0.0008

2.11. Event mean concentrations

Event mean concentrations (EMCs) were calculated for each TAC by pavement and experiment to compare results from this study with other studies and published toxicity information (e.g., LC50s). The following equation was used to calculate EMCs:

$$EMC = \frac{M}{V} = \frac{\sum C_i V_i}{\sum V_i} \quad (4)$$

where M is the total mass of a contaminant, V is the total effluent volume, C_i is the effluent concentration for composite I for a given pavement and experiment, and V_i is the effluent volume for composite i for a given pavement and experiment.

2.12. Evaluating 6PPDQ leaching from retained cTPs

Particles retained within the permeable pavement void spaces could potentially continue to leach 6PPDQ during subsequent storm events. To evaluate if effluent 6PPDQ concentrations were leached from cTPs trapped within the pavement matrix or leached from cTPs within the effluent sample, we examined the correlation between effluent cTPs and effluent 6PPDQ concentrations using linear regression with 6PPDQ concentration as the dependent variable. A significant positive relationship would suggest that cTPs within effluent samples drove 6PPDQ concentrations. In contrast, a lack of a positive relationship would suggest that 6PPDQ was leaching from cTPs retained within the pavement.

3. Results

3.1. Pavement hydrology

All four pavements tested had unique hydrological responses to dosing by synthetic storms, which was expected given their unique

Table 2
Influent and effluent flow volumes (L) during each of the 3 experimental storms for each pavement type. AC = asphalt + CCFCMs, AN = asphalt, CC = concrete + CCFCMs, and CN = concrete.

Pavement	Experiment	Influent volume (L)	Effluent volume (L)	Influent/effluent (ratio)
AC	1	12573	47	268
	2	7453	108	69
	3	6604	137	48
AN	1	5793	282	21
	2	4897	663	7
	3	4649	629	7
CC	1	2633	1119	2
	2	2511	1535	2
	3	2621	1588	2
CN	1	3298	739	5
	2	3402	717	5
	3	3306	660	5

structural and hydrologic character. Specifically, the influent volume required to produce effluent flow and the amount of effluent captured by the underdrain pipe differed for every pavement. During the synthetic storm dosing of the pavements, asphalt pavements took at least twice as long to generate effluent flows in the underdrain compared with concrete pavements. The asphalt with CCFs (AC) pavement required the largest volume of influent (Table 2) and longest dosing time to produce measurable subsurface flow. Surface runoff observed on this pavement during dosing suggests that clogging may have contributed to the longer time to generate subsurface flow.

3.2. Experiment 1 - background cTP and chemical concentrations

Field blank concentrations represented a mean of 14 % (se ± 1.5 %) of effluent sample concentrations (Table S3). We did not use field blank data to correct effluent sample concentrations because this would introduce a systemic increase in contaminant mass reduction estimate. Therefore, our approach was conservative with respect to how it might impact results. Lab blank and field blank TWP concentration data are available in Table S5 and Table S6, respectively. cTP and TAC concentrations measured during Experiment 1 represented background levels. In general, Experiment 1 effluents contained the lowest pollutant concentrations among the three experiments. Background TP mass estimates in Experiment 1 effluent ranged from 0.14 g to 3.23 g (Fig. 5) across the four pavement types. cTP concentrations were generally highest at the start and decreased throughout Experiment 1 (Fig. 6). Effluent chemical concentrations were much lower in Experiment 1 than in Experiment 2 or 3 (Fig. 5). Event mean concentrations of 6PPDQ ranged from 0 to 0.0029 μg/L (Table 3). For the AC, CC, and CN pavements, the lowest effluent TP masses were observed in Experiment 1, confirming that our TP quantification methods could discern between background TPs and deposited cTPs (Fig. 5). In contrast, the AN pavement released higher TP masses in Experiment 1 than Experiment 2 (Fig. 5).

3.3. Mass reduction of TPs by permeable pavements

cTP mass reductions, when summed over the two dosing experiments - Experiments 2 & 3 – ranged from 96.4 % to 99.3 % for all pavements (Fig. 5). Most cTP particles were observed in the effluent during Experiment 3, ranging from 1.08 g to 14.03 g across the four pavements. During Experiment 2, effluent cTP masses ranged from 2.47 g to 8.34 g. The highest effluent cTP mass was observed in the concrete pavements during Experiment 2, while the asphalt pavements released the highest effluent cTP masses during Experiment 3.

3.4. Tire additive chemicals in effluent

The TAC with the highest average EMC across all pavements in effluent stormwater was 2-OHBT, while 5-MBTR was the lowest of all 10 TACs measured (Table 3). 6PPDQ was the 8th highest EMC and ranged from 0 to 0.042 μg/L (Table 3). Effluent samples were dominated by 2-OHBT, DCU, HMMM, and DPG (Fig. 5). Correlation analysis showed that concentrations in effluent samples of HMMM, DPG, DCU, 24MoBT, and 2-OHBT were all strongly correlated (r values >0.9, adj. p-values <0.05) with each other across all pavements and experiments (Fig. S3). The same list of chemicals and NCBA were also significantly and strongly correlated with the effluent cTP mass (r values >0.71, adj. p-values <0.05) (Fig. S3). 6PPDQ was moderately correlated with NCBA, DPG, 24MoBT, HMMM, 2-OHBT, and DCU (r values 0.56–0.65, adjusted p-values <0.05) and was most strongly correlated with DPG (r = 0.64, adjusted p-values <0.05) and HMMM (r = 0.65, adjusted p-values <0.05).

3.5. Temporal dynamics of tire chemicals in effluent

The effluent's lowest concentrations of TACs and cTPs were consistently measured during Experiment 1 across all pavements (Table 3). These concentrations represented the ambient or background tire particles deposited by traffic in the school parking lot (Figs. 5 & 6) before

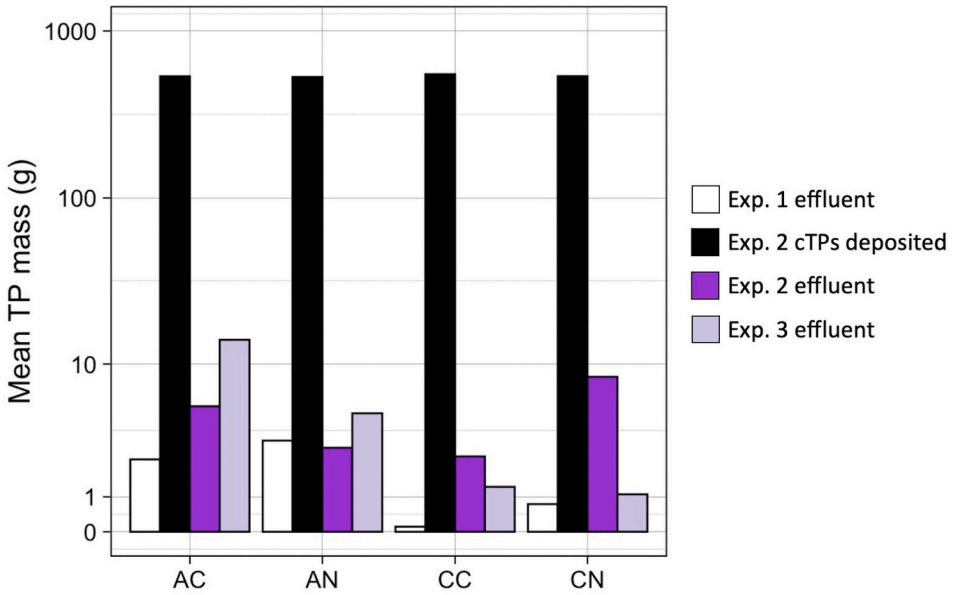

Fig. 5. Mass of tire particles (g) per pavement plotted on a log10 y-axis scale for Experiment 1 effluent, Experiment 2 deposition and effluent, and Experiment 3 effluent. cTPs were only added to the pavements for Experiment 2. All data shown here were corrected for effluent volume loss as described in Section 2.8.

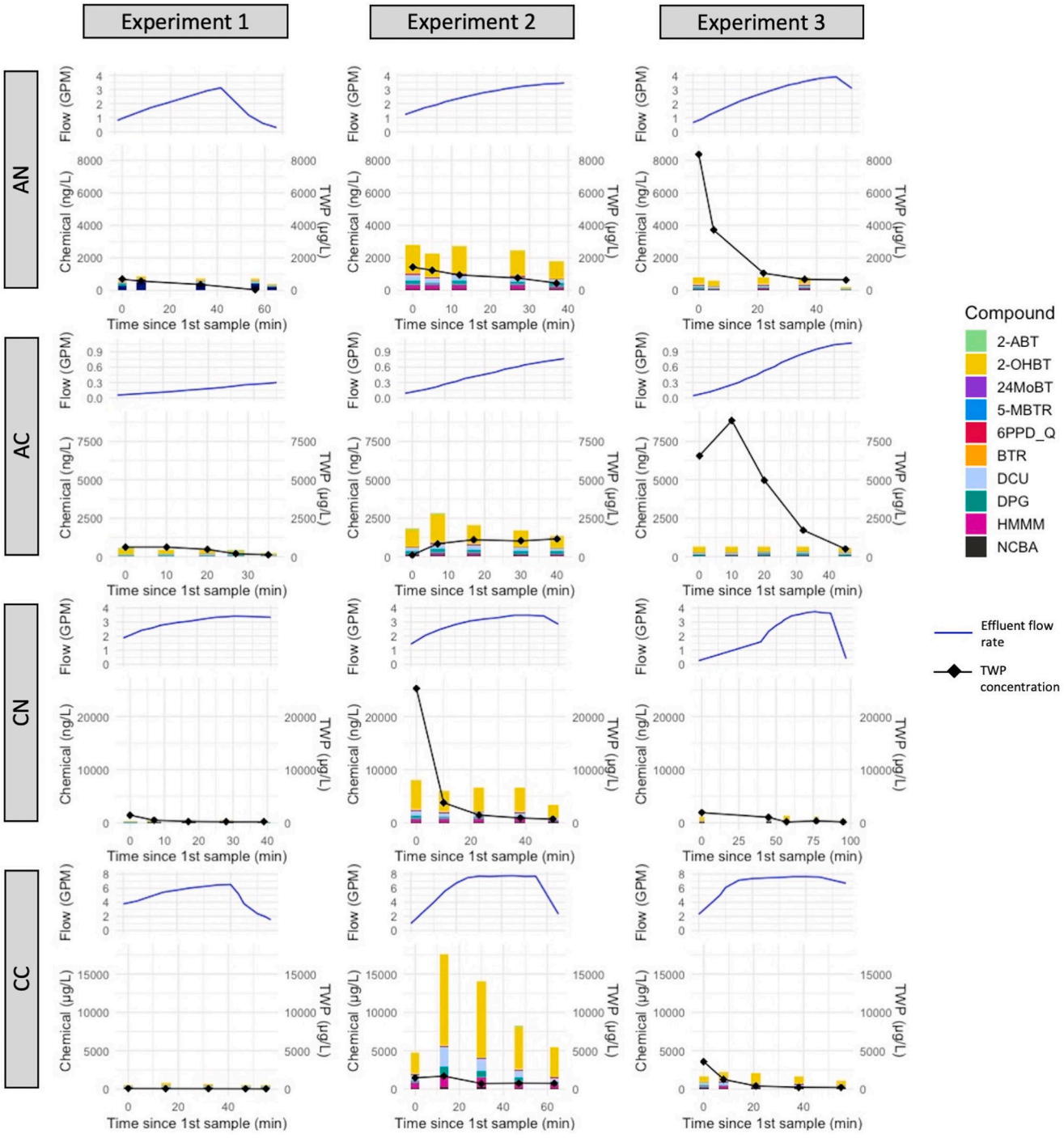

Fig. 6. Effluent flow rates (top), cTP, and chemical pollutographs (bottom) for each experiment and pavement in the study.

the running of our experiments. The concentrations of individual TACs were much higher in Experiment 2 following dry deposition of cTPs. TAC effluent concentrations during Experiment 3 were lower than Experiment 2 but higher than Experiment 1's baseline values (Table 3).

Peak tire chemical concentrations occurred on average 30 min before peak flow rates, where peak flows typically occurred midway or at the storm's end. The EMCs of the individual TACs did not appear to be driven by effluent flow rates or cTP concentrations. EMCs for all TACs typically peaked before cTP concentrations. In Experiment 2, EMCs peaked early except for the CN pavement (Fig. 6). For the CN pavement during Experiment 2, TAC concentrations peaked first, followed quickly by peak cTP concentrations. In Experiment 3, cTP concentrations consistently peaked before flow rates peaked (Fig. 6).

3.6. Estimated mass reduction of tire-associated chemicals

We observed mass reductions for most tire chemicals across all pavement types except for BTR and NCBA, which had effluent masses exceeding the estimated influent mass by up to 332 µg and 27 µg, respectively. Mass reductions ranged from 14 % to 100 % across all pavements and chemicals when the pavements showed treatment. Asphalt PPs (40 % - 95 %) had higher mass reductions for most TACs than concrete PPs (14 % -100 %, Table 4). Removal rates for the CC pavement were notably lower than other pavements for all chemicals

Table 3
Event mean concentrations (μg/L) of tire additive chemicals in pavement effluent samples ordered from left to right by highest average EMC to lowest.

Pavement	Experiment	Chemical event mean concentrations (μg/L)									
		2-OHBT	DCU	DPG	HMMM	NCBA	24MoBT	2-ABT	6PPDQ	5-MBTR	BTR
AC	1	0.251	0.062	0.078	0.004	0.004	0.012	0.013	0.003	0.003	0.002
AC	2	1.156	0.196	0.231	0.115	0.072	0.020	0.014	0.015	0.000	0.004
AC	3	0.337	0.058	0.145	0.031	0.042	0.015	0.01	0.007	0.000	0.003
AN	1	0.203	0.047	0.085	0.007	0.006	0.024	0.008	0.001	0.001	0.001
AN	2	1.578	0.29	0.253	0.209	0.094	0.024	0.013	0.026	0.001	0.002
AN	3	0.428	0.061	0.102	0.060	0.04	0.020	0.007	0.000	0.001	0.001
CC	1	0.324	0.106	0.22	0.000	0.033	0.027	0.008	0.000	0.000	0.000
CC	2	8.404	1.450	0.733	1.142	0.202	0.079	0.026	0.042	0.008	0.003
CC	3	1.187	0.212	0.219	0.133	0.079	0.025	0.017	0.004	0.001	0.003
CN	1	0.218	0.065	0.050	0.000	0.027	0.023	0.008	0.000	0.002	0.002
CN	2	4.332	0.720	0.400	0.490	0.156	0.046	0.022	0.000	0.000	0.004
CN	3	0.804	0.139	0.102	0.084	0.067	0.014	0.014	0.000	0.003	0.002
Average		1.602	0.284	0.218	0.190	0.043	0.027	0.013	0.008	0.002	0.002

Table 4
Mass reduction of tire chemicals by permeable pavements expressed as a percentage in descending order of average reductions across all pavements. Values take into account effluent volume corrections described in Section 2.8.

Chemical	% Mass reduction by pavement				Average
	AC	AN	CC	CN	
5-MBTR	95	90	64	81	83
6PPDQ	52	66	55	100	68
DPG	66	80	60	71	69
HMMM	87	85	47	68	72
2-ABT	36	67	47	37	47
2-OHBT	74	78	23	44	55
DCU	72	76	14	41	51
24MoBT	40	50	18	35	36
NCBA	−42	−6	−61	−77	−47
BTR	−334	−15	−91	−154	−148

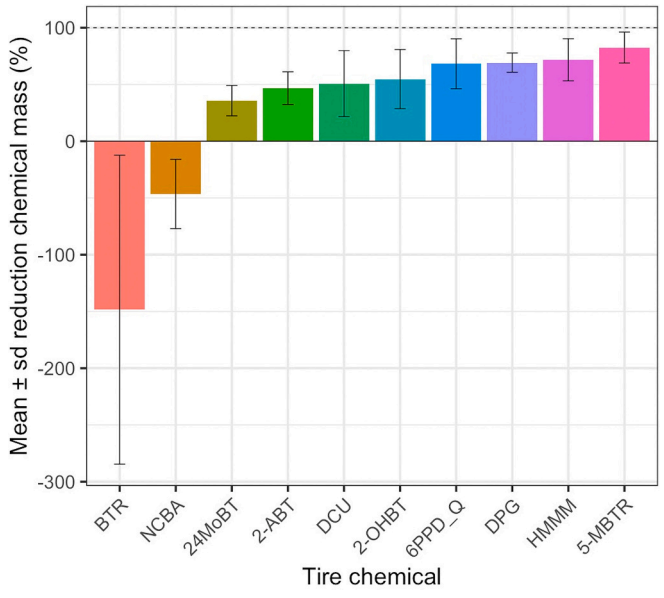

Fig. 7. Estimated % mass reduction, averaged across pavements, of tire-associated chemicals over Experiments 2 and 3 following tire particle deposition. Error bars represent +/− the standard deviation of the mean. Effluent masses were corrected for volume loss, as described in Section 2.9.

(−16.2 % - 78.3 %). The mean mass reduction of 6PPDQ was 68 % (range 52 % - 100 %; Table 4). 6PPDQ was not detected in any effluent sample from the CN pavement, so mass reductions were considered 100 % for that pavement. Estimated reductions are presented in Fig. 7.

3.7. Leaching of 6PPD quinone from retained tire particles

Linear regression models were used to explain 6PPDQ variance with cTP concentrations to infer if cTP concentrations were adequate predictors of in-situ 6PPDQ concentrations. Our results showed no relationship by regression modeling in Experiment 1 ($r^2 = 0.000021$, $p = 0.99$; Fig. 8). However, there was a weakly positive but insignificant relationship in Experiment 2 ($r^2 = 0.065$, $p = 0.36$). However, during Experiment 3, a linear regression model explained over 66 % of the variance of 6PPDQ concentrations in effluent flows with cTP concentrations ($r^2 = 0.61$, $p < 0.001$).

4. Discussion

4.1. Influence of pavement type on pollutant treatment

We observed differences in the treatment of cTPs and TACs across the studied pavements, which may be attributable to differences in pavement structure and location. Despite high rates of cTP removal observed across all pavements, the majority of effluent cTPs emerged from the concrete pavements earlier than the asphalt pavements. We hypothesize this difference in timing is related to higher infiltration rates in concrete pavements and therefore quicker transport through pavement profile. Generally, infiltration rates of pervious concrete sections tend to be higher than porous asphalt sections exposed to similar traffic conditions (Houle et al., 2010). Additionally, lower infiltration rates on the asphalt pavements from this study may reflect the location of the asphalt pavements next to an impervious parking lot area, producing run-on flows and particulates that might be clogging the porous asphalt pavements at a greater rate than the previous concrete sections.

Another compounding issue was that the centroids of the cTP dosing areas were farther away from the effluent collection location for asphalt pavements than for the concrete pavements. The dosing centroid for asphalt pavements were 28.7 and 29.8 m from their effluent sampling points, while both concrete section dosing centroids were only 4.8 m. Therefore, it may have simply taken longer for cTPs to reach the subsurface effluent sampling location with the asphalt pavements. Additionally, the AN and CN pavements were located by the entrances to the

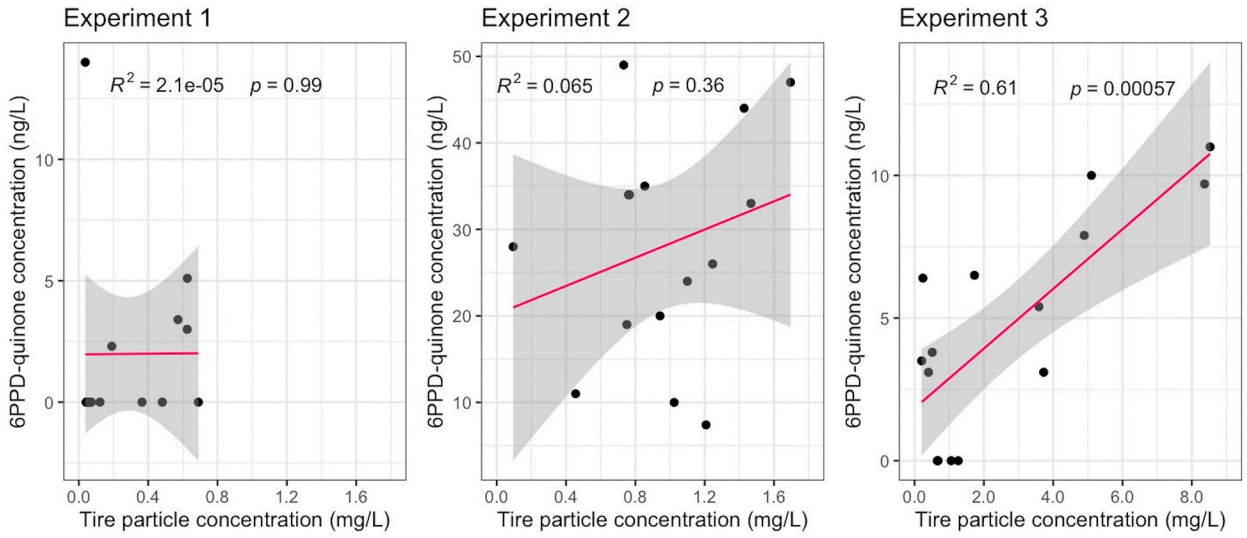

Fig. 8. Correlations between tire particle concentration and 6PPDQ concentration using Pearson's correlation coefficient. Data from the CN pavement is not included here because all samples from this pavement were below the method detection limit for 6PPDQ. Note that x and y-axes have different scales across experiment panels.

study site and were likely exposed to higher vehicle acceleration and braking than the other pavement sections. Since higher vehicle acceleration and braking increase the rate of TWP deposition (Wik and Dave, 2009), the higher Experiment 1 effluent mass in the AN and CN pavements (Fig. 4) compared to the AC and CC pavements may reflect these higher deposition rates. The proximity of AN and CN pavements to the impervious pavements surrounding the experimental sites may also have led to increased deposition of particles tracked in from the impervious pavements.

Differences in TAC mass reductions across the pavements may also be attributable to the structural differences between the concrete and asphalt pavements. Higher mass reduction of TACs was generally observed in the asphalt pavements compared to the concrete pavements. The study asphalt pavements had longer effluent travel distances and lower infiltration rates, so they likely had higher hydraulic retention times (HRT) than concrete pavements. In a hydraulic tracer study previously conducted on these pavements, the time to peak for the mass of a dissolved tracer (KBr) to pass the effluent sampler was longer for asphalt pavements (AC = 30 min, AN = 17 min) than concrete pavements (CC = 16 min, CN = 12 min). Longer HRTs are associated with enhanced adsorption (Muthu et al., 2017), which may have contributed to the improved removal of TACs by the asphalt pavements.

4.2. Tire particle retention and transport through pavements

Despite depositing approximately 500 g of cTPs on each pavement in Experiment 2, <19 g of cTPs (corrected for effluent volume loss) were estimated to have exited the systems via the effluent pipe from each pavement (Experiments 2 and 3), suggesting that the remaining cTP mass was retained within the pavement void spaces. This finding supports our hypothesis that permeable pavements could treat tire particles by mechanisms similar to the treatment of suspended sediments - retained at varying efficiencies depending on particle size (Jayakaran et al., 2019). These results are also consistent with the findings of Rasmussen et al. (2023), who suggested that permeable pavements may be a significant environmental sink for tire particles. Similarly, Brown et al. (2009) reported high TSS removal rates from 90 to 96 % by porous asphalt pavements and noted that effluent sediments were finer than influent sediments, suggesting better retention of coarser sediments. They also noted that solids removal occurred throughout the layers of the permeable pavement structure. Still, the most significant "sieving action" occurred at the interface of the geotextile membrane overlying the subbase soils.

Assuming that cTPs were removed via similar mechanisms to sediments in permeable pavements, they were likely retained in void spaces throughout the system and possibly settled onto the impermeable geomembrane. Given that the cTPs used in this study were highly hydrophobic (average contact angle = 127.9°), they likely partitioned out of the water and preferentially adsorbed to non-aqueous surfaces within the pavement's profile.

Importantly, tire particles retained within permeable pavements could be removed through regular maintenance (Rasmussen et al., 2023), helping to divert them from environmental compartments like soils and water. Maintaining infiltration rates in permeable pavements requires regular maintenance (Drake et al., 2013). Maintenance involves vacuum sweeping and sometimes pressure washing to remove particles from the wearing layer of the pavement (Winston et al., 2016). By removing these particles, TRWP and hydrophobic organic contaminants sorbed to particle surfaces will also be removed, thereby effecting the removal of toxic contaminants.

Our cTP effluent mass estimates incorporate some uncertainty because we used image analyses to infer cTPs in the effluent and did not weigh effluent particles directly. The imaging analysis relied on identifying cTPs using a thresholding function to select only the darkest particles on a grayscale image and then filter the selected particles to size and circularity ranges that omitted filaments and larger dark particles (often bits of asphalt). This imaging process and the assumptions about cTP volume and density could have underestimated the actual tire particle mass in the effluent samples. However, all microplastic identification methods rely on assumptions that impact quantification or bias results (Zarfl, 2019).

4.3. Tire additive chemicals

The chemicals dominating the tire additive chemical profiles in pavement effluents (2-OHBT, DCU, DPG, and HMMM) were consistent with reports of dominant tire-associated chemicals in stormwater and snowmelt runoff (Challis et al., 2021) and in surface water (Rauert et al., 2022) samples in a creek receiving runoff after storm events. These chemicals comprise rubber vulcanizing agents (HMMM and DPG) and reaction byproducts associated with tire rubber production (DCU and 2-OHBT). When the effluent mass was less than the influent mass (TAC treatment), TAC mass reductions ranged from 14 % to 100 % across pavements. Given the pavements' relatively short hydraulic residence

times, this suggests a rapid adsorption process was the removal mechanism. However, two TACs (BTR and NCBA) had greater masses at the effluent than the influent (TAC export), suggesting that the pavement matrix inherently contained a source of the chemicals. NCBA has a relatively high log K_{ow} (4.23, Kumata et al., 2002) and may have sorbed to sediments/surfaces and accumulated from previous pavement use. All the other TACs were organic compounds with some hydrophobic properties. We hypothesize that the sorption was likely driven by hydrophobic interactions with the internal pavement surface and other organic matter, such as microbial biofilms (Newman et al., 2006) within the pavement matrix.

4.4. Leaching of tire chemicals from retained particles

Regression modeling shows that 6PPDQ concentrations from Experiments 1 and 2 could not be explained with observed cTPs concentrations in the effluent. However, in Experiment 3, cTPs concentrations were a good predictor of the variability in 6PPDQ concentrations. Also, 6PPDQ concentrations were elevated following TP deposition in Experiment 2, suggesting leaching from retained particles drove 6PPDQ concentrations in Experiment 2. The strong and significant relationship between 6PPDQ and cTP in pavement effluents from Experiment 3 suggests that leaching from particles retained in the pavements was greatly reduced by Experiment 3. This finding suggests that without additional cTP inputs and prolonged exposure to stormwater, the leaching of TACs from cTPs appears to taper off. This is important because permeable pavements are typically connected hydraulically to downstream receiving waters and sometimes groundwater through the native subbase soils. However, we acknowledge that more replication of these experiments is needed to elucidate further the long-term fate and transport of cTPs in permeable pavements beyond 3 days.

4.5. Implications for adoption of permeable pavements for stormwater management

In this study, we have shown that permeable pavements can mitigate tire particles and tire-associated chemical pollution. Historically, the adoption of permeable pavements has been hampered by the lower resistance to mechanical wear compared with traditional pavements. Additionally, retrofitting existing impermeable surfaces with permeable pavements is expensive. The amending permeable pavement with CCFCMs to increase strength suggests we can address this first limitation with existing technologies.

The Infrastructure Investment and Jobs Act ($1.2 trillion in funding) contains discretionary funds of $500 million over the next five years for the *Healthy Streets Program*, which provides funds for deploying *cool* pavements (U.S. Environmental Protection Agency, 2012) and permeable pavements to mitigate urban heat islands and flooding from stormwater runoff (Lindenberg, 2021). Given this sizeable federal investment in permeable pavements, the financial barrier mentioned previously will be easier to overcome. We, therefore, believe this to be an opportune time to install permeable pavements as a GSI intervention for addressing tire wear particles and 6PPDQ pollution where they are released into the environment.

5. Conclusions

The results of a short study that explored background levels of tire particles and tire associated chemicals, followed by a single impulse of cTPs on four pavements suggest that permeable pavements are effective in mitigating tire particles and their associated chemicals. Given the limitations of idealized particles, and limited replication, our data show that over 96 % of the tire particle mass that was applied to the surface of four pavements, was retained. The pavements also demonstrated the removal of most tire-associated contaminants (14–100 %), except NCBA and BTR, which were exported (−6 % to −334 %). Regression analyses between 6PPDQ and cTP concentrations suggested that 6PPDQ leached from cTPs were retained in the pavement matrix following deposition. Still, this leaching stopped by Experiment 3 when most 6PPDQ concentrations could be explained by cTPs mass in the effluent. Permeable pavements provide an opportunity to mitigate tire-associated pollution at its generation source. Additionally, the required routine maintenance of permeable pavements presents an additional mechanism to remove tire particles and associated pollutants from the urban ecosystem.

Funding

This work was supported as gift funds donated to Washington State University by the Boeing Company to support the permeable pavements project at the IDEA School in Tacoma, Washington.

CRediT authorship contribution statement

Chelsea J. Mitchell: Conceptualization, Methodology, Software, Formal analysis, Data curation, Writing – original draft, Visualization, Writing – review & editing. **Anand D. Jayakaran:** Conceptualization, Methodology, Validation, Writing – review & editing, Supervision, Project administration, Funding acquisition.

Declaration of competing interest

The authors declare the following financial interests/personal relationships which may be considered as potential competing interests: Anand Jayakaran reports financial support was provided as gift funds by The Boeing Company. Approval of this work by The Boeing Company was not sought or expected.

Data availability

Data will be made available on request.

Acknowledgments

We thank the Boeing Company, specifically Lori Blair and Shyla Miller for championing and creating the funding basis for this work. We are grateful to the City of Tacoma (Jessica Knickerbocker, Angela Gallardo), and IDEA High School (Zach Varnell, Kainoa Higgins) for supporting this work. At Washington State University, Dr. Jen McIntyre helped us conceptualize our methods and analyses of tire-associated chemicals. Drs. Somayeh Nassiri and Karl Englund were critical to constucting the test pavements. Brandon Boyd designed and built the pavement dosing system, supported the fieldwork and performed the majority of WP extraction. Carly Thompson maintained all site instrumentation and assisted with all fieldwork. Dr. Valerie Holm supported scanning electron microscopy. Lastly, Benjamin Leonard helped with image analysis.

Appendix A. Supplementary data

Supplementary data to this article can be found online at https://doi.org/10.1016/j.scitotenv.2023.168236.

References

Baensch-Baltruschat, B., Kocher, B., Stock, F., Reifferscheid, G., 2020. Tyre and road wear particles (TRWP) - a review of generation, properties, emissions, human health risk, ecotoxicity, and fate in the environment. Sci. Total Environ. 733, 137823 https://doi.org/10.1016/j.scitotenv.2020.137823.

Boucher, J., Friot, D., 2017. Primary Microplastics in the Oceans: A Global Evaluation of Sources. IUCN International Union for Conservation of Nature [accessed 2022 May 24]. https://portals.iucn.org/library/node/46622.

Bright Singh, S., Madasamy, M., 2022. Investigation of aggregate size effects on properties of basalt and carbon fibre-reinforced pervious concrete. Road Mater.

Pavement Des. 23 (6), 1305–1328. https://doi.org/10.1080/14680629.2021.1886158.
Brinkmann, M., Montgomery, D., Selinger, S., Miller, J.G.P., Stock, E., Alcaraz, A.J., Challis, J.K., Weber, L., Janz, D., Hecker, M., et al., 2022. Acute toxicity of the tire rubber-derived chemical 6PPD-quinone to four fishes of commercial, cultural, and ecological importance. Environ. Sci. Technol. Lett. 9 (4), 333–338. https://doi.org/10.1021/acs.estlett.2c00050.
Brown, C., Chu, A., Van Duin, B., Valeo, C., 2009. Characteristics of sediment removal in two types of permeable pavement. Water Qual. Res. J. 44 (1), 59–70. https://doi.org/10.2166/wqrj.2009.007.
Capolupo, M., Sørensen, L., Jayasena, K.D.R., Booth, A.M., Fabbri, E., 2020. Chemical composition and ecotoxicity of plastic and car tire rubber leachates to aquatic organisms. Water Res. 169, 115270 https://doi.org/10.1016/j.watres.2019.115270.
Challis, J.K., Popick, H., Prajapati, S., Harder, P., Giesy, J.P., McPhedran, K., Brinkmann, M., 2021. Occurrences of Tire rubber-derived contaminants in cold-climate urban runoff. Environ. Sci. Technol. Lett. 8 (11), 961–967. https://doi.org/10.1021/acs.estlett.1c00682.
Drake, J.A.P., Bradford, A., Marsalek, J., 2013. Review of environmental performance of permeable pavement systems: state of the knowledge. Water Qual. Res. J. 48 (3), 203–222. https://doi.org/10.2166/wqrjc.2013.055.
Du, B., Tian, Z., Peter, K.T., Kolodziej, E.P., Wong, C.S., 2020. Developing unique nontarget high-resolution mass spectrometry signatures to track contaminant sources in urban waters. Environ. Sci. Technol. Lett. 7 (12), 923–930. https://doi.org/10.1021/acs.estlett.0c00749.
Ebrahimian, A., Wadzuk, B., Traver, R., 2019. Evapotranspiration in green stormwater infrastructure systems. Sci. Total Environ. 688, 797–810. https://doi.org/10.1016/j.scitotenv.2019.06.256.
Ebrahimian, A., Sample-Lord, K., Wadzuk, B., Traver, R., 2020. Temporal and spatial variation of infiltration in urban green infrastructure. Hydrol. Process. 34 (4), 1016–1034. https://doi.org/10.1002/hyp.13641.
Gupta, A., Rodriguez-Hernandez, J., Castro-Fresno, D., 2019. Incorporation of additives and fibers in porous asphalt mixtures: a review. Materials 12 (19), 3156. https://doi.org/10.3390/ma12193156.
Hidalgo-Ruz, V., Gutow, L., Thompson, R.C., Thiel, M., 2012. Microplastics in the marine environment: a review of the methods used for identification and quantification. Environ. Sci. Technol. 46 (6), 3060–3075.
Hiki, K., Yamamoto, H., 2022. Concentration and leachability of N-(1, 3-dimethylbutyl)-N′-phenyl-p-phenylenediamine (6PPD) and its quinone transformation product (6PPD-Q) in road dust collected in Tokyo, Japan. Environ. Pollut. 302, 119082.
Hou, F., Tian, Z., Peter, K.T., Wu, C., Gipe, A.D., Zhao, H., Alegria, E.A., Liu, F., Kolodziej, E.P., 2019. Quantification of organic contaminants in urban stormwater by isotope dilution and liquid chromatography-tandem mass spectrometry. Anal. Bioanal. Chem. 411 (29), 7791–7806. https://doi.org/10.1007/s00216-019-02177-3.
Houle, K.M., Roseen, R.M., Ballestero, T.P., Briggs, J.F., Houle, J.J., 2010. Examinations of Pervious Concrete and Porous Asphalt Pavements Performance for Stormwater Management in Northern Climates. Low Impact Development.
Jayakaran, A., Knappenberger, T., Stark, J., Hinman, C., 2019. Remediation of stormwater pollutants by porous asphalt pavement. Water 11 (3), 520. https://doi.org/10.3390/w11030520.
Johannessen, C., Helm, P., Metcalfe, C.D., 2021. Detection of selected tire wear compounds in urban receiving waters. Environ. Pollut. 287, 117659 https://doi.org/10.1016/j.envpol.2021.117659.
Kole, P.J., Löhr, A.J., Van Belleghem, F., Ragas, A., 2017. Wear and tear of tyres: a stealthy source of microplastics in the environment. IJERPH 14 (10), 1265. https://doi.org/10.3390/ijerph14101265.
Kumata, H., Yamada, J., Masuda, K., Takada, H., Sato, Y., Sakurai, T., Fujiwara, K., 2002. Benzothiazolamines as tire-derived molecular markers: sorptive behavior in street runoff and application to source apportioning. Environ. Sci. Technol. 36 (4), 702–708. https://doi.org/10.1021/es0155229.
Lane, E.W., 1947. Report of the subcommittee on sediment terminology. Trans AGU 28 (6), 936. https://doi.org/10.1029/TR028i006p00936.
LeFevre, G.H., Hozalski, R.M., Novak, P.J., 2012. The role of biodegradation in limiting the accumulation of petroleum hydrocarbons in raingarden soils. Water Res. 46 (20), 6753–6762. https://doi.org/10.1016/j.watres.2011.12.040.
Li, H., Davis, A.P., 2008. Urban particle capture in bioretention media. I: laboratory and field studies. J. Environ. Eng. 134 (6), 409–418. https://doi.org/10.1061/(ASCE)0733-9372(2008)134:6(409).
Lindenberg, T., 2021. What's in it for the Concrete Pavement Industry?.
Maes, T., Jessop, R., Wellner, N., Haupt, K., Mayes, A.G., 2017. A rapid-screening approach to detect and quantify microplastics based on fluorescent tagging with Nile Red. Sci. Rep. 7 (1), 44501.
McIntyre, J.K., Davis, J.W., Incardona, J.P., Stark, J.D., Anulacion, B.F., Scholz, N.L., 2014. Zebrafish and clean water technology: assessing soil bioretention as a protective treatment for toxic urban runoff. Sci. Total Environ. 500–501, 173–180. https://doi.org/10.1016/j.scitotenv.2014.08.066.
McIntyre, J.K., Davis, J.W., Hinman, C., Macneale, K.H., Anulacion, B.F., Scholz, N.L., Stark, J.D., 2015. Soil bioretention protects juvenile salmon and their prey from the toxic impacts of urban stormwater runoff. Chemosphere 132, 213–219. https://doi.org/10.1016/j.chemosphere.2014.12.052.
McIntyre, J.K., Edmunds, R.C., Anulacion, B.F., Davis, J.W., Incardona, J.P., Stark, J.D., Scholz, N.L., 2016. Severe coal tar sealcoat runoff toxicity to fish is prevented by bioretention filtration. Environ. Sci. Technol. 50 (3), 1570–1578. https://doi.org/10.1021/acs.est.5b04928.
McIntyre, J.K., Prat, J., Cameron, J., Wetzel, J., Mudrock, E., Peter, K.T., Tian, Z., Mackenzie, C., Lundin, J., Stark, J.D., et al., 2021. Treading water: tire wear particle leachate recreates an urban runoff mortality syndrome in Coho but not chum Salmon. Environ. Sci. Technol. 55 (17), 11767–11774. https://doi.org/10.1021/acs.est.1c03569.
Meyer, J.L., Paul, M.J., Taulbee, W.K., 2005. Stream ecosystem function in urbanizing landscapes. J. N. Am. Benthol. Soc. 24 (3), 602–612. https://doi.org/10.1899/04-021.1.
Monaghan, J., Jaeger, A., Agua, A.R., Stanton, R.S., Pirrung, M., Gill, C.G., Krogh, E.T., 2021. A direct mass spectrometry method for the rapid analysis of ubiquitous tire-derived toxin N -(1,3-dimethylbutyl)- N ′-phenyl- p -phenylenediamine quinone (6-PPDQ). Environ. Sci. Technol. Lett. 8 (12), 1051–1056. https://doi.org/10.1021/acs.estlett.1c00794.
Muthu, M., Santhanam, M., Kumar, M., 2017. Effect of hydraulic retention time on the filtration performance of porous concrete. Adv. Const. Mater. Syst. 2, 195–200.
Nassiri, S., AlShareedah, O., Rodin, H., Englund, K., 2021. Mechanical and durability characteristics of pervious concrete reinforced with mechanically recycled carbon fiber composite materials. Mater. Struct. 54 (3), 107. https://doi.org/10.1617/s11527-021-01708-8.
Newman, A.P., Coupe, S.J., Smith, H.G., Puehmeier, T., Bond, P., 2006. The Microbiology of Permeable Pavements.
Parker-Jurd, F.N.F., Napper, I.E., Abbott, G.D., Hann, S., Thompson, R.C., 2021. Quantifying the release of tyre wear particles to the marine environment via multiple pathways. Mar. Pollut. Bull. 172, 112897 https://doi.org/10.1016/j.marpolbul.2021.112897.
Peter, K.T., Tian, Z., Wu, C., Lin, P., White, S., Du, B., McIntyre, J.K., Scholz, N.L., Kolodziej, E.P., 2018. Using high-resolution mass spectrometry to identify organic contaminants linked to urban stormwater mortality syndrome in Coho Salmon. Environ. Sci. Technol. 52 (18), 10317–10327. https://doi.org/10.1021/acs.est.8b03287.
Pratt, C.J., Newman, A.P., Bond, P.C., 1999. Mineral oil bio-degradation within a permeable pavement: long term observations. Water Sci. Technol. 39 (2), 103–109. https://doi.org/10.1016/S0273-1223(99)00013-X.
Rangelov, M., Nassiri, S., Haselbach, L., Englund, K., 2016. Using carbon fiber composites for reinforcing pervious concrete. Constr. Build. Mater. 126, 875–885. https://doi.org/10.1016/j.conbuildmat.2016.06.035.
Rasmussen, L.A., Lykkemark, J., Andersen, T.R., Vollertsen, J., 2023. Permeable pavements: a possible sink for tyre wear particles and other microplastics? Sci. Total Environ. 869, 161770 https://doi.org/10.1016/j.scitotenv.2023.161770.
Rauert, C., Charlton, N., Okoffo, E.D., Stanton, R.S., Agua, A.R., Pirrung, M.C., Thomas, K.V., 2022. Concentrations of tire additive chemicals and tire road wear particles in an Australian urban tributary. Environ. Sci. Technol. 56 (4), 2421–2431. https://doi.org/10.1021/acs.est.1c07451.
Rauert, C., Charlton, N., Okoffo, E.D., Stanton, R.S., Agua, A.R., Pirrung, M.C., Thomas, K.V., 2022. Concentrations of tire additive chemicals and tire road wear particles in an Australian urban tributary. Environ. Sci. Technol. 56 (4), 2421–2431. https://doi.org/10.1021/acs.est.1c07451.
Renner, G., Nellessen, A., Schwiers, A., Wenzel, M., Schmidt, T.C., Schram, J., 2019. Data preprocessing & evaluation used in the microplastics identification process: a critical review & practical guide. TrAC Trends Anal. Chem. 111, 229–238.
Rodgers, T.F.M., Wang, Y., Humes, C., Jeronimo, M., Johannessen, C., Spraakman, S., Giang, A., Scholes, R.C., 2023 Jun 16. Bioretention cells provide a 10-fold reduction in 6PPD-Quinone mass loadings to receiving waters: evidence from a field experiment and modeling. Environ. Sci. Technol. Lett. https://doi.org/10.1021/acs.estlett.3c00203 acs.estlett.3c00203.
Rodin, H., Rangelov, M., Nassiri, S., Englund, K., 2018. Enhancing mechanical properties of pervious concrete using carbon fiber composite reinforcement. J. Mater. Civ. Eng. 30 (3), 04018012 https://doi.org/10.1061/(ASCE)MT.1943-5533.0002207.
Rodrigues, M.O., Gonçalves, A.M.M., Gonçalves, F.J.M., Abrantes, N., 2020. Improving cost-efficiency for MPs density separation by zinc chloride reuse. MethodsX 7, 100785. https://doi.org/10.1016/j.mex.2020.100785.
Roseen, R., Ballestero, T., Houle, J., Briggs, J., Houle, K., 2012. Water quality and hydrologic performance of a porous asphalt pavement as a stormwater treatment strategy in a cold climate. J. Environ. Eng. 138, 81–89. https://doi.org/10.1061/(ASCE)EE.1943-7870.0000459.
Schneider, C.A., Rasband, W.S., Eliceiri, K.W., 2012. NIH Image to ImageJ: 25 years of image analysis. Nat. Methods 9 (7), 671–675. https://doi.org/10.1038/nmeth.2089.
Scholz, M., Grabowiecki, P., 2007. Review of permeable pavement systems. Build. Environ. 42 (11), 3830–3836. https://doi.org/10.1016/j.buildenv.2006.11.016.
Selbig, W.R., Buer, N., Danz, M.E., 2019. Stormwater-quality performance of lined permeable pavement systems. J. Environ. Manag. 251, 109510 https://doi.org/10.1016/j.jenvman.2019.109510.
Sharma R, Malaviya P. 2021. Management of stormwater pollution using green infrastructure: the role of rain gardens WIREs Water 8(2). doi:https://doi.org/10.1002/wat2.1507. [accessed 2023 Jun 16]. https://doi.org/10.1002/wat2.1507.
Smyth, K., Drake, J., Li, Y., Rochman, C., Van Seters, T., Passeport, E., 2021. Bioretention cells remove microplastics from urban stormwater. Water Res. 191, 116785 https://doi.org/10.1016/j.watres.2020.116785.
Tagg, A.S., Sapp, M., Harrison, J.P., Ojeda, J.J., 2015. Identification and quantification of microplastics in wastewater using focal plane array-based reflectance micro-FT-IR imaging. Anal. Chem. 87 (12), 6032–6040.
Tian, Z., Zhao, H., Peter, K.T., Gonzalez, M., Wetzel, J., Wu, C., Hu, X., Prat, J., Mudrock, E., Hettinger, R., et al., 2021. A ubiquitous tire rubber–derived chemical induces acute mortality in coho salmon. Science 371 (6525), 185–189. https://doi.org/10.1126/science.abd6951.
Tian, Z., Gonzalez, M., Rideout, C.A., Zhao, H.N., Hu, X., Wetzel, J., Mudrock, E., James, C.A., McIntyre, J.K., Kolodziej, E.P., 2022. 6PPD-quinone: revised toxicity

assessment and quantification with a commercial standard. Environ. Sci. Technol. Lett. 9 (2), 140–146. https://doi.org/10.1021/acs.estlett.1c00910.
U.S. Environmental Protection Agency. Reducing urban heat islands: Compendium of strategies. Draft. https://www.epa.gov/heat-islands/heat-island-compendium.
Vietz, G.J., Walsh, C.J., Fletcher, T.D., 2016. Urban hydrogeomorphology and the urban stream syndrome: treating the symptoms and causes of geomorphic change. Prog. Phys. Geogr.: Earth Environ. 40 (3), 480–492. https://doi.org/10.1177/0309133315605048.
Wadell, H., 1932. Volume, shape, and roundness of rock particles. J. Geol. 40 (5), 443–451. https://doi.org/10.1086/623964.
Wagner, S., Klöckner, P., Reemtsma, T., 2022. Aging of tire and road wear particles in terrestrial and freshwater environments – a review on processes, testing, analysis and impact. Chemosphere 288, 132467. https://doi.org/10.1016/j.chemosphere.2021.132467.
Walsh, C.J., Roy, A.H., Feminella, J.W., Cottingham, P.D., Groffman, P.M., Morgan, R.P., 2005. The urban stream syndrome: current knowledge and the search for a cure. J. N. Am. Benthol. Soc. 24 (3), 706–723.
Werbowski, L.M., Gilbreath, A.N., Munno, K., Zhu, X., Grbic, J., Wu, T., Sutton, R., Sedlak, M.D., Deshpande, A.D., Rochman, C.M., 2021. Urban stormwater runoff: a major pathway for anthropogenic particles, black rubbery fragments, and other types of microplastics to urban receiving waters. ACS EST Water 1 (6), 1420–1428. https://doi.org/10.1021/acsestwater.1c00017.
Wik, A., 2007. Toxic components leaching from tire rubber. Bull. Environ. Contam. Toxicol. 79 (1), 114–119. https://doi.org/10.1007/s00128-007-9145-3.
Wik, A., Dave, G., 2009. Occurrence and effects of tire wear particles in the environment – a critical review and an initial risk assessment. Environ. Pollut. 157 (1), 1–11. https://doi.org/10.1016/j.envpol.2008.09.028.
Winston, R.J., Al-Rubaei, A.M., Blecken, G.T., Viklander, M., Hunt, W.F., 2016. Maintenance measures for preservation and recovery of permeable pavement surface infiltration rate–The effects of street sweeping, vacuum cleaning, high pressure washing, and milling. J. Environ. Manage. 169, 132–144.
Zarfl, C., 2019. Promising techniques and open challenges for microplastic identification and quantification in environmental matrices. Anal. Bioanal. Chem. 411 (17), 3743–3756. https://doi.org/10.1007/s00216-019-01763-9.
Zhang, K., Lim, J., Nassiri, S., Englund, K., Li, H., 2019. Reuse of carbon fiber composite materials in porous hot mix asphalt to enhance strength and durability. Case Stud. Constr. Mater. 11, e00260 https://doi.org/10.1016/j.cscm.2019.e00260.
Zhu, X., Munno, K., Grbic, J., Werbowski, L.M., Bikker, J., Ho, A., Guo, E., Sedlak, M., Sutton, R., Box, C., et al., 2021. Holistic assessment of microplastics and other anthropogenic microdebris in an urban bay sheds light on their sources and fate. ACS EST Water 1 (6), 1401–1410. https://doi.org/10.1021/acsestwater.0c00292.
Ziajahromi, S., Drapper, D., Hornbuckle, A., Rintoul, L., Leusch, F.D.L., 2020. Microplastic pollution in a stormwater floating treatment wetland: detection of tyre particles in sediment. Sci. Total Environ. 713, 136356 https://doi.org/10.1016/j.scitotenv.2019.136356.